ACS APPLIED MATERIALS & INTERFACES

Research Article

Cite This: ACS Appl. Mater. Interfaces 2018, 10, 15200−15206

www.acsami.org

Polyacrylamide Gel-Contained Zinc Finger Peptide as the "Lock" and Zinc Ions as the "Key" for Construction of Ultrasensitive Prostate-Specific Antigen SERS Immunosensor

Linglin Xie, Xia Yang, Yi He, Ruo Yuan,* and Yaqin Chai*

Key Laboratory of Luminescent and Real-Time Analytical Chemistry, Ministry of Education, College of Chemistry and Chemical Engineering, Southwest University, Chongqing 400715, People's Republic of China

Supporting Information

ABSTRACT: In this work, we adopted polyacrylamide gel-contained zinc finger peptide (PZF) as a "lock" of Raman signal and zinc ions (Zn^{2+}) as a sensitive "key", which was converted from target-captured ZnO NPs, to achieve the measurement of prostate-specific antigen (PSA). Owing to the lock effect from PZF, the surface-enhanced Raman scattering (SERS) tag toluidine blue (TB) connected on Ag NP-coating silica wafer was sheltered leading to low Raman response. Meanwhile, target PSA can specifically connect with antibody 2-coupled ZnO nanocomplexes ($ZnO@Au@Ab_2$) and antibody 1-coupled magnetic ($CoFe_2O_4@Au@Ab_1$) nanocomposite through sandwich immunoassay. In the presence of HCl, the ZnO NPs would convert into Zn^{2+} to open the PZF because Zn^{2+} can specifically react with zinc finger peptide to destroy the PZF structure forming abundant pores. In this way, Zn^{2+} could act as the key of Raman signal to open the PZF structure obtaining a strong Raman signal of TB. The proposed SERS sensor can have a quantitative detection of PSA within the range of 1 pg mL^{-1} to 10 ng mL^{-1} with a detection limit of 0.65 pg mL^{-1}. The interaction between zinc finger peptide and Zn^{2+} was firstly applied in SERS sensor for the sensitive detection of PSA. These results demonstrated that the new designed SERS biosensor could be a promising tool in biomarker diagnosis.

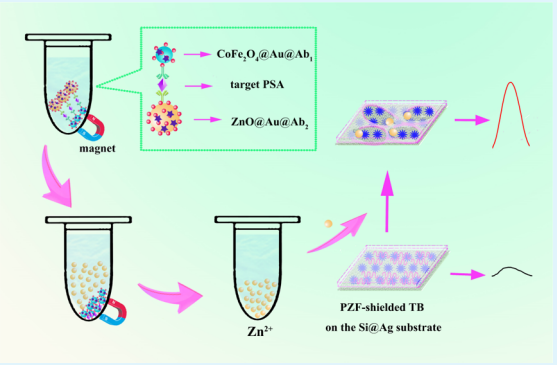

KEYWORDS: *prostate-specific antigen (PSA), polyacrylamide gel-contained zinc finger peptide (PZF), surface-enhanced Raman scattering (SERS), zinc finger peptide−Zn^{2+} recognition, sandwich immunoassay*

INTRODUCTION

Surface-enhanced Raman scattering (SERS) is well known for its good specificity,[1] high sensitivity,[2] and superior biocompatibility,[3] resulting in the broad use of SERS-based immunoassays for analyzing biomaterials,[4−6] such as proteins, disease biomarkers, cells, etc. Usually, the usage of excellent metallic substrate[7−9] and the application of DNA cycle amplification[10,11] could be utilized in SERS-assisted sensors to achieve the signal improvement to some extent, sadly holding deficiencies such as time consumption or complicated operation. Thus, it is a challenge to find a simple and more sensitive method for signal amplification in SERS-based bioassays. Herein, we utilized zinc finger peptide (PZF)[12−14] as the "lock" to vastly block the Raman signal and Zn^{2+} converted from target-captured ZnO NPs as the "key" to recover the Raman signal. This key could open the lock to destroy the polyacrylamide gel structure for the interaction between zinc finger peptide and Zn^{2+}, ultimately achieving the exposure of the SERS tag toluidine blue (TB) to realize a stronger Raman intensity.

Being the most common visceral cancer among older male population, prostate cancer[15,16] is a core zone of cancer biomarker study. Prostate-specific antigen (PSA) is a well-known and the most commonly used cancer biomarker,[17,18] tested in serum and plasma of sufferers for the preoperative screening and diagnosis of prostatic carcinoma. Hence, early and precise detection of PSA for prostate cancer diagnosis can be equipped with great medical value. Nowadays, a growing number of immunosensors based on the utilization of novel nanomaterials[19−22] have been reported and could detect PSA sensitively, and the sensitivity of PSA detection still has space to improve.

In this paper, a SERS biosensor utilizing a novel PZF as signal lock and Zn^{2+} as signal switch was designed to sensitively detect PSA. First, the SERS tag toluidine blue (TB) was connected to the Ag NP-coating silicon wafer to obtain SERS substrate (Si@Ag@TB) with a strong Raman signal. Then, the PZF was dropped on the Si@Ag@TB to shield TB, resulting in an appreciable decrease of Raman signal. Next, $ZnO@Au@Ab_2$ specifically recognized target PSA after adding $CoFe_2O_4@Au@$

Received: December 27, 2017
Accepted: April 16, 2018
Published: April 16, 2018

DOI: 10.1021/acsami.7b19717
ACS Appl. Mater. Interfaces 2018, 10, 15200−15206

Scheme 1. (A) Capture of Target PSA Based on Sandwich Immunoassay; (B) Conversion of PSA-Captured ZnO Nanoparticles into Zn^{2+}; and (C) Schematic Graph of the Proposed SERS Platform

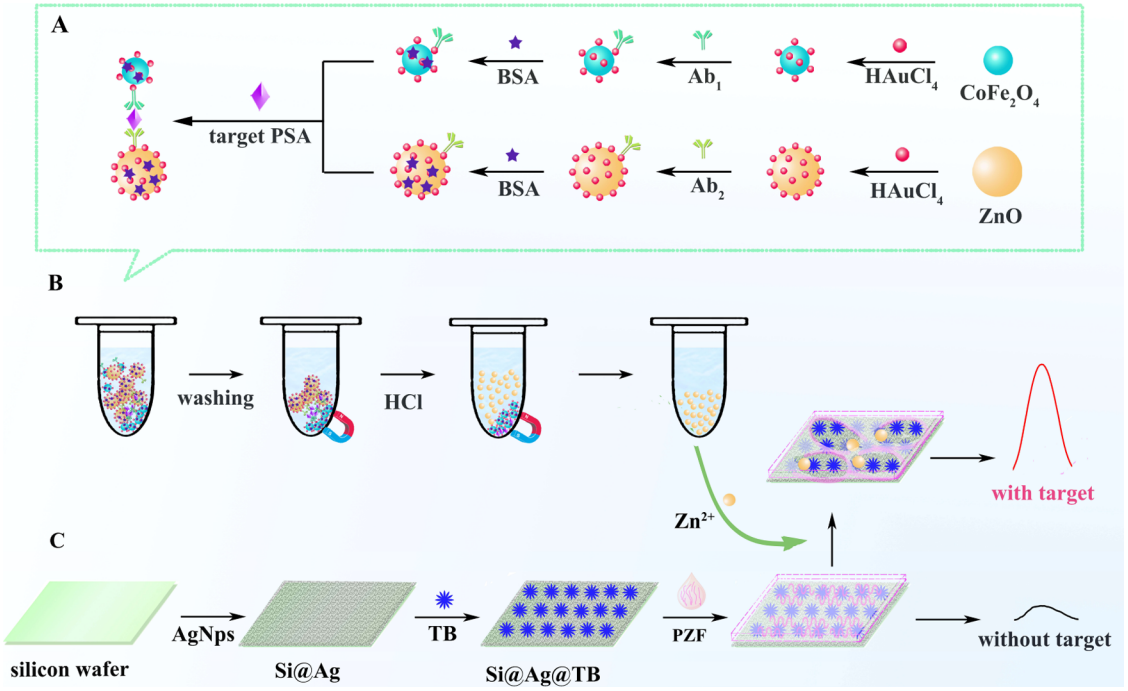

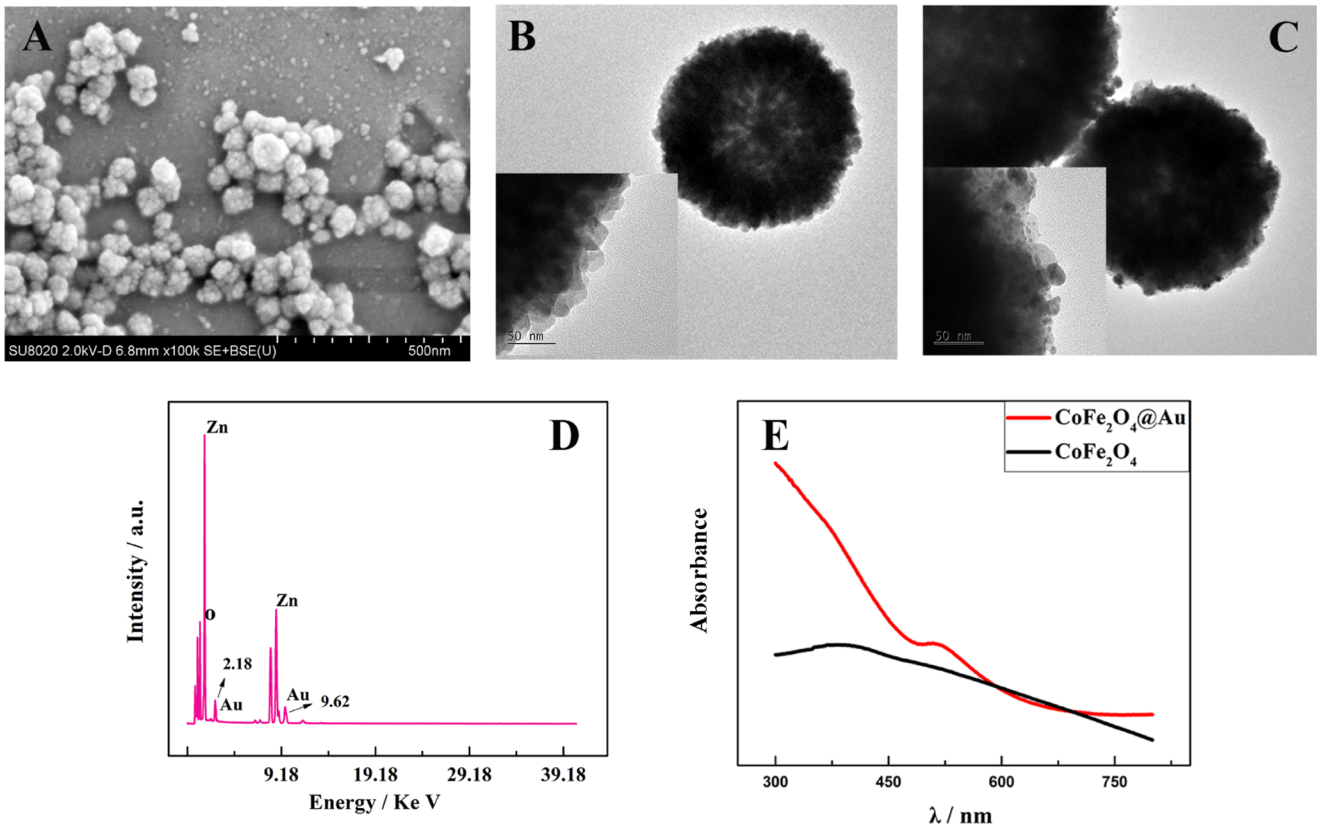

Figure 1. (A) SEM graph of $CoFe_2O_4$; (B) TEM graph of ZnO, inset: magnified graph of (B); (C) TEM graph of ZnO@Au, inset: enlarged graph of (C); (D) Energy-dispersive spectrum of ZnO@Au; and (E) UV−vis spectra of $CoFe_2O_4$ (black) and $CoFe_2O_4$@AuNPs (red).

Ab_1 to acquire the sandwich structure, which was further dissolved by hydrochloric acid to convert ZnO into Zn^{2+}. Then, the obtained Zn^{2+} was added to PZF-covering Si@Ag@TB to specifically combine with zinc finger peptide, which will form many pores for the exposure of TB. In this way, we could obtain a high Raman response. And Scheme 1 showed the fabrication of our SERS immunosensor. The proposed method could obtain a broad linear range and low limit of detection in

DOI: 10.1021/acsami.7b19717
ACS Appl. Mater. Interfaces 2018, 10, 15200−15206

the sensitive detection of PSA, holding great potential in biomedical research and clinical diagnostics. And this method also provided a new way of signal improvement of SERS-based immunosensor.

EXPERIMENTAL SECTION

Preparation of ZnO@Au@Ab$_2$. ZnO nanosphere was synthesized with the method developed by Wang and co-workers.[23] The precipitate was collected via centrifugal separation at 12 000 rpm for 10 min and washed with ultrapure water and ethyl alcohol alternately before drying.

The obtained ZnO nanospheres were used as reactants to synthesize the ZnO@Au composite via the protocol presented in the previous literature.[24] And the purple deposit can be collected by centrifugal separation before storage at 4 °C. ZnO@Au@Ab$_2$ was prepared by blending 2 mL of ZnO@Au solution and 2 mL of Ab$_2$ under mild stirring at 4 °C for 12 h, and the acquired ZnO@Au@Ab$_2$ was washed several times to remove redundant Ab$_2$ before being stored at 4 °C.

Synthesis of $CoFe_2O_4$@Au@Ab$_1$. $CoFe_2O_4$ nanoparticles were produced using the scheme proposed by Dong and co-workers.[25] After the washing and collection of deposited $CoFe_2O_4$, the obtained $CoFe_2O_4$ was redispersed into ultrapure water and used as the reactant in the preparation of $CoFe_2O_4$@Au nanocomposite. And $CoFe_2O_4$@Au nanocomposite was synthesized according to the literature.[26] The product ($CoFe_2O_4$@Au) was obtained via centrifugation at 8000 rpm for 15 min and washed several times. Thereafter, 2 mL of Ab$_1$ was added to 2 mL of solution containing $CoFe_2O_4$@Au nanocomposite under mild magnetic stirring for 12 h at 4 °C to acquire $CoFe_2O_4$@Au@Ab$_1$ and excess Ab$_1$ was removed by centrifugal washing.

Preparation of the PZF and SERS Substrate (Si@Ag@TB). The PZF was prepared based on the literature with slight modification.[27] First, 0.14 g of acrylamide and 0.01 g of bisacrylamide were dissolved in 1 mL of phosphate buffer under gentle stirring for 10 min. Subsequently, 0.1 mL of 5 μM zinc finger peptide was added with continuous stirring. Second, 0.05 mL of tetramethylethylenediamine and 0.10 g of $(NH_4)_2S_2O_8$ were dispersed into 1 mL of ultrapure water to form the coagulant; 20 μL of this coagulant was added into the previous mixture with mild stirring for 2 min and then the PZF was stored at 4 °C.

The Si@Ag substrate was obtained according to the literature.[28] Then, the prepared Si@Ag wafer was immersed into 1 mL of 0.3 mM TB to acquire the SERS substrate; finally, 5 μL of PZF was added on the SERS substrate (Si@Ag@TB) to lock the Raman signal of TB, which was stored at 37 °C.

SERS-Biosensor Assay Procedure. $CoFe_2O_4$@Au@Ab$_1$ (5 μL) and ZnO@Au@Ab$_2$ (5 μL) were mixed with 2 μL of BSA (1 mg mL^{-1}) for 30 min to close the active sites. Subsequently, 5 μL of PSA of different concentrations was first mixed with $CoFe_2O_4$@Au@Ab$_1$@BSA and the obtained complex was mixed with ZnO@Au@Ab$_2$@BSA for reacting for 50 min at 37 °C to form immune sandwich structure. The resultant sandwich complex was separated via magnetic separation, and 5 μL of 0.1 M HCl was added to turn PSA-captured ZnO NPs into Zn^{2+}. Finally, the obtained Zn^{2+} was added on the PZF-covering SERS substrate to react with zinc finger peptide for recovering the Raman signal of TB.

RESULTS AND DISCUSSION

Characterization of Obtained Materials. Scanning electron microscopy (SEM) image for the Ag NP-coating silicon wafer is shown in Figure S1, in which Ag nanospheres were uniformly distributed on the silicon wafer. Figure 1A reveals that $CoFe_2O_4$ nanoparticles had spherical-like shape with a diameter of 50 nm. The SEM image (Figure S2) revealed that ZnO particles were spherical with a diameter of approximately 1 μm. After AuNPs were assembled on the ZnO nanosphere surface, the SEM image (Figure S3) demonstrated that the morphology and size of ZnO@Au were almost unchanged compared with ZnO; from inset images (Figure 1B,C), we can find that many Au nanoparticles were distributed uniformly on the external surface of ZnO nanosphere. Following the energy-dispersive spectrum of the ZnO@Au (Figure 1D), we could find that the peaks of Zn and O elements appear and the atomic ratio of Zn/O is approximate to 1:1. The signal response of Au appeared at around 2.18 and 9.62 keV. As illustrated in Figure 1E, compared with the UV spectrum of $CoFe_2O_4$ (black), the spectrum of $CoFe_2O_4$@Au (red) roundly exhibited a peak at 560 nm. This peak could be ascribed to the collective surface plasmonic resonance of the embedded AuNPs,[29] which confirmed that the $CoFe_2O_4$@Au was successfully prepared.

Principle of the SERS-Assisted Biosensor. Some essential experiments were used to evaluate the feasibility of our protocol, and related results are shown in Figure 2. When

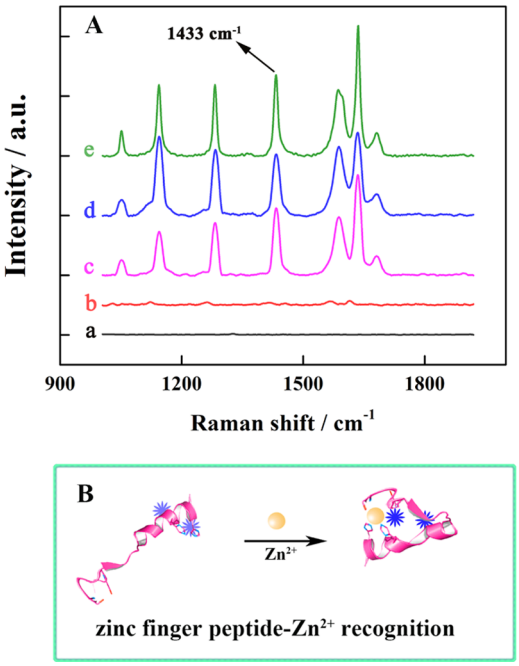

Figure 2. (A) (a) SERS spectra of Si@Ag; (b) SERS spectra of Si@Ag@TB after PZF was added on the substrate; (c) SERS spectra of PZF-covering Si@Ag@TB after Zn^{2+} converted from PSA-captured ZnO NPs was added on the substrate; (d) SERS spectra of PZF-covering Si@Ag@TB after 0.1 M Zn^{2+} was directly added on the substrate, and (e) SERS spectra of Si@Ag@TB. (B) Schematic diagram for the interaction between polyacrylamide gel-contained zinc finger peptide and Zn^{2+}.

TB was dropped on the Si@Ag (Figure 2, curve e), we could find the most obvious peak of TB at 1433 cm^{-1} compared to the SERS spectra of Si@Ag (Figure 2, curve a). When PZF was added onto Si@Ag@TB to shield the Raman signal of TB (lock state), the Raman intensity of TB at 1433 cm^{-1} could be barely measured (Figure 2, curve b). However, after combining with PSA (10 ng mL^{-1}), the Zn^{2+} obtained from PSA-captured ZnO NPs was added on the PZF-covering Si@Ag@TB. Thus, a strong Raman signal (Figure 2, curve c) was obtained, illustrating that the Raman signal of TB was recovered ("opening" state). When 0.1 M Zn^{2+} was directly added on the PZF-covering substrate, we could see that an obvious Raman peak appeared (Figure 2, curve d), which is similar to

DOI: 10.1021/acsami.7b19717
ACS Appl. Mater. Interfaces 2018, 10, 15200−15206

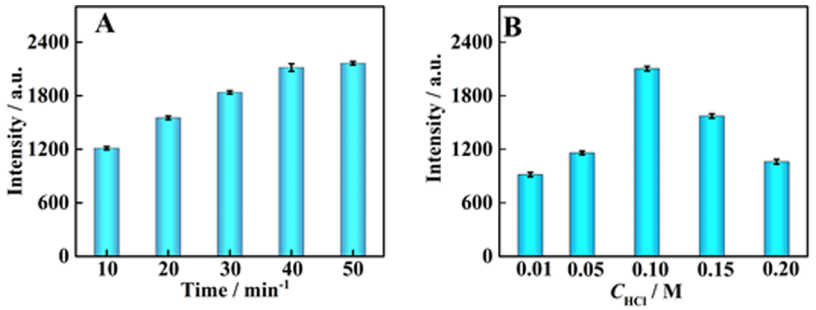

Figure 3. (A) Optimization of the incubation time on the Raman intensity of TB. (B) Optimization of HCl concentration on the Raman intensity of TB.

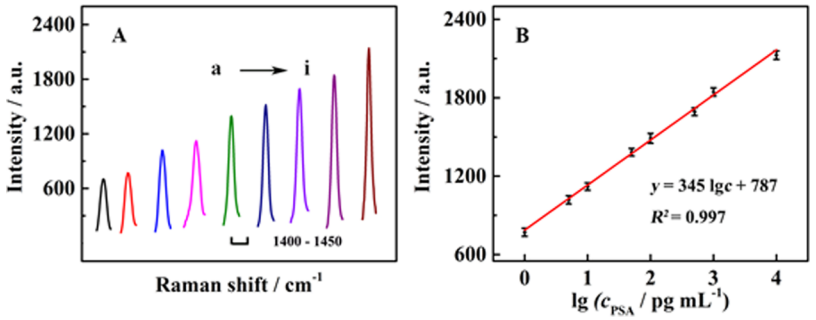

Figure 4. (A) SERS spectra of the proposed immunosensor with the addition of PSA (pg mL^{-1}) from a to i: 0, 1, 5, 10, 50, 100, 500, 1000, and 10 000. (B) The calibration curve of Raman intensity at 1433 cm^{-1} against lg *c*.

curve b, which further confirmed that Zn^{2+} converted from the PSA-captured ZnO NPs in our designed biosensor could open the polyacrylamide gel-contained zinc finger peptide for recovering the Raman signal of TB to achieve the sensitive detection. The interaction between zinc finger peptide and Zn^{2+} is shown in Figure 2B; the cysteine and histidine in the zinc finger peptide could bind with Zn^{2+} with the folding of the polypeptide chain to form a small hydrophobic core for the exposure of TB, and so the Raman signal of TB can be detected in this way.

Optimization of Conditions. To assure the proper performance of the SERS-based biosensor, testing conditions, including HCl concentration and the incubation time of the capture of PSA, via sandwich immunoassay were investigated in this study. Figure 3A shows the Raman intensity of TB at 1433 cm^{-1}, which reached a steady value when incubation time was 40 min. To insure complete capture of PSA, we selected 50 min as the optimizing time to capture PSA. As illustrated in Figure 3B, when the concentration of HCl was 0.1 M, the Raman response of TB at 1433 cm^{-1} reached the maximum. The decrease of Raman intensity with the increasing of HCl concentration could be attributed to the destruction of zinc finger peptide, which would affect the pore formation and further have influence on the Raman intensity of TB. For maximizing the sensitivity of the proposed biosensor, we chose 0.1 M as the optimal HCl concentration.

SERS-Based Protocol Performance. To confirm the analytical performance to detect PSA based on this immunosensor, we detected PSA with different concentrations (1 pg mL^{-1} to 10 ng mL^{-1}) under the best conditions. Figure 4A indicates that the Raman response at 1433 cm^{-1} was gradually increasing following the increasing concentration of PSA. Figure 4B indicates a linear correlation between the Raman peak intensity of TB at 1433 cm^{-1} and the logarithm of PSA concentration, with regression equation as $y = 345 \lg c + 787$ (y refers to the Raman peak intensity and c refers to the concentration of PSA), and the square of correlation coefficient was 0.997 with the detection limit as low as 0.65 pg mL^{-1}. Each concentration was measured three times to assure its accuracy. Here, the detection limit for PSA calculation was tailored to IUPAC recommendation, namely, LOD = $3n/m$ (n is the standard deviation of Raman response without target PSA (n = 11) and m refers to the slope of the relevant calibration curve).[30]

Table 1 indicates that our immunosensor can obtain superior sensitivity and broader detection range, so this SERS biosensor-based zinc finger peptide–Zn^{2+} recognition could achieve the efficient measurement of PSA.

Table 1. Performance Comparison of Different Kinds of PSA Sensors

analytical method	detection limit (pg mL^{-1})	linear range (ng mL^{-1})	refs
PEC	3	0.01–80	31
ULISA	1.2	0.01–1	32
ELISA	16.0	0.2–6.4	33
ECL	590	0–10	34
ELISA	0.165	0.002–0.064	35
SERS	590	1–50	36
SERS	0.65	0.001–10	this work

Reproducibility of the SERS-Based Platform. Here, 15 various spots of SERS spectra were studied on the same substrate at 1433 cm^{-1} for evaluation of the reproducibility in the immunosensor. Figure 5A,B indicates that the SERS spectra of 15 different spots were nearly the same and the coefficient of variation was about 6%. We measured five different substrates at a PSA concentration of 100 pg mL^{-1}, and the results are

DOI: 10.1021/acsami.7b19717
ACS Appl. Mater. Interfaces 2018, 10, 15200–15206

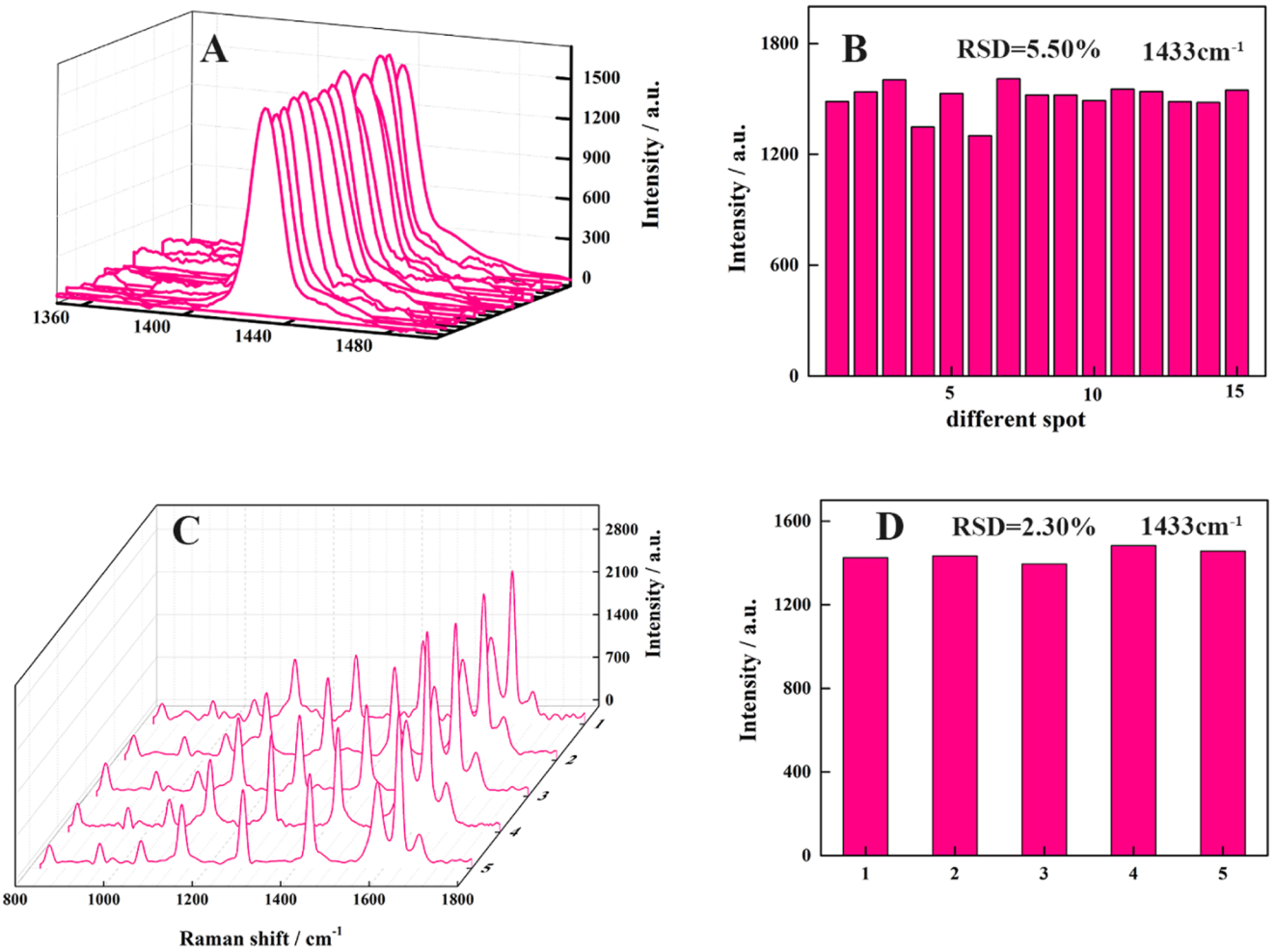

Figure 5. (A) SERS spectra of 15 different spots on the same substrate from 1350 to 1600 cm^{-1} and (B) relevant histogram of the Raman peak intensity at 1433 cm^{-1} (c_{PSA} = 100 pg mL^{-1}). (C) SERS spectra of five different substrates under the same condition (c_{PSA} = 100 pg mL^{-1}) and (D) relevant histogram for the Raman peak intensity at 1433 cm^{-1} of five different SERS substrates.

displayed in Figure 5C,D. The corresponding RSD for different SERS substrates was 2.30%. Moreover, after cold storage for 2 weeks, 90% of the original response of PSA under the same concentration could be still obtained, which is shown in Figure S4. These results showed that the devised immunosensor could have a good reproducibility.

Selective Ability of the Immunosensor. Selectivity is essential for the immunosensor for PSA detection; herein, we chose human alpha-fetoprotein (AFP), carcinoembryonic antigen (CEA), and bovine serum albumin (BSA) as interferences to verify the selectivity of the proposed biosensor. Figure 6 indicates that no dramatic change of the Raman peak intensity at 1433 cm^{-1} with comparison to the blank test was observed when 10 ng mL^{-1} of AFP, CEA, and BSA were added. However, when AFP, CEA, and BSA were mixed with PSA (every interference was 10 ng mL^{-1} except PSA was 100 pg mL^{-1}), the Raman intensity of the mixture was almost similar with the result that only PSA existed, which indicated that our immunosensor could achieve the specific detection of PSA.

Application of the Proposed SERS-Based Sensor. We diluted different concentrations of PSA with healthy human serum sample to measure the recovery experiment. The obtained results are shown in Table 2, and we could find that the proposed immunosensor obtained good recoveries from 98.10 to 102.4% and RSD values were from 1.0 to 3.4%. These

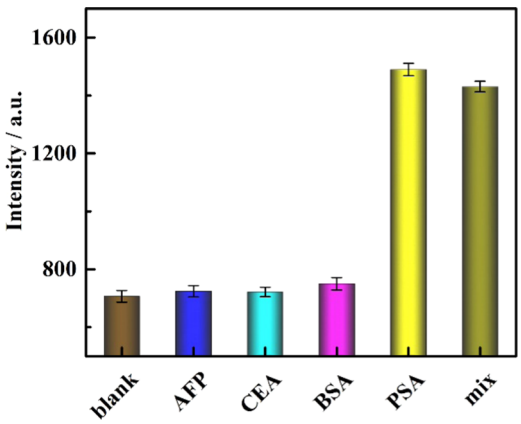

Figure 6. Selectivity of the SERS-based biosensor for PSA detection against other interferences.

results showed that our immunosensor could be used in clinical analysis.

CONCLUSIONS

In summary, we described a novel SERS-assisted immunosensor combined with zinc finger peptide interaction with Zn^{2+} in signal amplification for PSA detection. This proposed

DOI: 10.1021/acsami.7b19717
ACS Appl. Mater. Interfaces 2018, 10, 15200−15206

Table 2. Detection of PSA Diluted in Human Blood Serum (n = 3)

serum sample	concentration of PSA added (pg mL^{-1})	concentration obtained with immunosensor (pg mL^{-1})	recovery (%)	RSD (%)
1	10	10.24	102.4	1.0
2	50	49.97	99.95	3.4
3	100	98.10	98.10	1.0
4	500	492.3	98.46	3.2
5	1000	1005.9	100.6	3.3

method can achieve the detection limit of 0.65 pg mL^{-1} and a detection range from 1 pg mL^{-1} to 10 ng mL^{-1}. The good performance of the biosensor was attributed to the following reasons. First, the PZF was introduced into SERS-assisted biosensor, which served as the lock of signal, for exclusive reaction with Zn^{2+} to improve the specificity of the biosensor. Second, the Zn^{2+} converted from the target PSA-captured ZnO NPs served as switch in the signal amplification and specifically interacted with zinc finger peptide for further improving the sensitivity. Moreover, the proposed SERS-assisted sensor performed high sensitivity, stability, and wide linear range in PSA detection, exhibiting that this original method could achieve accurate detection of other analytes. It is noteworthy that this work found a new path in signal improvement of SERS biosensors as well as a novel protein-cooperative assay for biomarker analysis.

■ ASSOCIATED CONTENT

Supporting Information

The Supporting Information is available free of charge on the ACS Publications website at DOI: 10.1021/acsami.7b19717.

Reagents and material, apparatus and measurements, SEM graph of substrate Ag NP-coating silicon wafer, SEM graph of ZnO, SEM graph of ZnO@Au, and stability of the biosensor (PDF)

■ AUTHOR INFORMATION

Corresponding Authors

*E-mail: yuanruo@swu.edu.cn. Tel: +86-23-68252277. Fax: +86-23-68253172 (R.Y.).

*E-mail: yqchai@swu.edu.cn (Y.C.).

ORCID

Ruo Yuan: 0000-0003-3664-6236

Notes

The authors declare no competing financial interest.

■ ACKNOWLEDGMENTS

This project has been financially supported by the NNSF of China (21775124, 21575116, and 21675129), the Fundamental Research Funds for the Central Universities, China (XDJK2015C099 and SWU114079), China Postdoctoral Science Foundation (2015M572427), and Chongqing Postdoctoral Research Project (xm2015019).

■ REFERENCES

(1) Zheng, J.; Jiao, A.; Yang, R.; Li, H.; Li, J.; Shi, M.; Ma, C.; Jiang, Y.; Deng, L.; Tan, W. Fabricating a Reversible and Regenerable Raman-Active Substrate with a Biomolecule-Controlled DNA Nanomachine. *J. Am. Chem. Soc.* **2012**, *134*, 19957−19960.

(2) Sharma, B.; Ma, K.; Glucksberg, M. R.; Van Duyne, R. P. Seeing through Bone with Surface-Enhanced Spatially Offset Raman Spectroscopy. *J. Am. Chem. Soc.* **2013**, *135*, 17290−17293.

(3) Han, X. X.; Ji, W.; Zhao, B.; Ozaki, Y. Semiconductor-Enhanced Raman Scattering: Active Nanomaterials and Applications. *Nanoscale* **2017**, *9*, 4847−4861.

(4) Hu, Y.; Cheng, H.; Zhao, X.; Wu, J.; Muhammad, F.; Lin, S.; He, J.; Zhou, L.; Zhang, C.; Deng, Y.; Wang, P.; Zhou, Z.; Nie, S.; We, H. Surface-Enhanced Raman Scattering Active Gold Nanoparticles with Enzyme-Mimicking Activities for Measuring Glucose and Lactate in Living Tissues. *ACS Nano* **2017**, *11*, 5558−5566.

(5) Xu, L.-J.; Lei, Z.-C.; Li, J. X.; Zong, C.; Yang, C. Y. J.; Ren, B. Label-Free Surface-Enhanced Raman Spectroscopy Detection of DNA with Single-Base Sensitivity. *J. Am. Chem. Soc.* **2015**, *137*, 5149−5154.

(6) Lin, L.; Tian, X.; Hong, S.; Dai, P.; You, Q.; Wang, R.; Feng, L.; Xie, C.; Tian, Z.-Q.; Chen, X. A Bioorthogonal Raman Reporter Strategy for SERS Detection of Glycans on Live Cells. *Angew. Chem., Int. Ed.* **2013**, *52*, 7266−7271.

(7) Zhou, X.; Xu, W.; Wang, Y.; Kuang, Q.; Shi, Y.; Zhong, L.; Zhang, Q. Fabrication of Cluster/Shell Fe_3O_4/Au Nanoparticles and Application in Protein Detection via a SERS Method. *J. Phys. Chem. C* **2010**, *114*, 19607−19613.

(8) Su, J.; Wang, D.; Nörbel, L.; Shen, J.; Zhao, Z.; Dou, Y.; Peng, T.; Shi, J.; Mathur, S.; Fan, C.; Song, S. Multicolor Gold−Silver Nano-Mushrooms as Ready-to-Use SERS Probes for Ultrasensitive and Multiplex DNA/miRNA Detection. *Anal. Chem.* **2017**, *89*, 2531−2538.

(9) Liu, H.-L.; Cao, J.; Hanif, S.; Yuan, C.; Pang, J.; Levicky, R.; Xia, X.-H.; Wang, K. Size-Controllable Gold Nanopores with High SERS Activity. *Anal. Chem.* **2017**, *89*, 10407−10413.

(10) Ma, S.; Li, Q.; Yin, Y.; Yang, J.; Liu, D. Interference-Free Surface-Enhanced Raman Scattering Tags for Single-Cell Molecular Imaging with a High Signal-to-Background Ratio. *Small* **2017**, *13*, No. 1603340.

(11) Zheng, J.; Hu, Y.; Bai, J.; Ma, C.; Li, J.; Li, Y.; Shi, M.; Tan, W.; Yang, R. Universal Surface-Enhanced Raman Scattering Amplification Detector for Ultrasensitive Detection of Multiple Target Analytes. *Anal. Chem.* **2014**, *86*, 2205−2212.

(12) Jiang, P.; Guo, Z. Fluorescent Detection of Zinc in Biological Systems: Recent Development on the Design of Chemosensors and Biosensors. *Coord. Chem. Rev.* **2004**, *248*, 205−229.

(13) Gan, X.; Sun, P.; Li, H.; Tian, X.; Zhang, B.; Wu, J.; Tian, Y.; Zhou, H. A Conveniently Prepared and Hypersensitized Small Molecular Fluorescent Probe: Rapidly Detecting Free Zinc Ion in HepG2 cells and Arabidopsis. *Biosens. Bioelectron.* **2016**, *86*, 393−397.

(14) Deng, S.; Zhang, T.; Ji, X.; Wan, Y.; Xin, P.; Shan, D.; Zhang, X. Detection of Zinc Finger Protein (EGR1) Based on Electrogenerated Chemiluminescence from Singlet Oxygen Produced in a Nano-claySupported Porphyrin Environment. *Anal. Chem.* **2015**, *87*, 9155−9162.

(15) Li, C.; Curreli, M.; Lin, H.; Lei, B.; Ishikawa, F. N.; Datar, R.; Cote, R. J.; Thompson, M. E.; Zhou, C. Complementary Detection of Prostate-Specific Antigen Using In_2O_3 Nanowires and Carbon Nanotubes. *J. Am. Chem. Soc.* **2005**, *127*, 12484−12485.

(16) He, Y.; Xie, S.; Yang, X.; Yuan, R.; Chai, Y. Electrochemical Peptide Biosensor Based on in Situ Silver Deposition for Detection of Prostate Specific Antigen. *ACS Appl. Mater. Interfaces* **2015**, *7*, 13360−13366.

(17) Lu, N.; Gao, A.; Dai, P.; Mao, H.; Zuo, X.; Fan, C.; Wang, Y.; Li, T. Ultrasensitive Detection of Dual Cancer Biomarkers with Integrated CMOS-Compatible Nanowire Arrays. *Anal. Chem.* **2015**, *87*, 11203−11208.

(18) Kaya, T.; Kaneko, T.; Kojima, S.; Nakamura, Y.; Ide, Y.; Ishida, K.; Suda, Y.; Yamashita, K. High-Sensitivity Immunoassay with Surface Plasmon Field-Enhanced Fluorescence Spectroscopy Using a Plastic Sensor Chip: Application to Quantitative Analysis of Total Prostate-Specific Antigen and GalNAcβ1−4GlcNAc-Linked Prostate-Specific Antigen for Prostate Cancer Diagnosis. *Anal. Chem.* **2015**, *87*, 1797−1803.

(19) Akter, R.; Arrigan, D. W. M. Detection of Prostate Specific Membrane Antigenat Picomolar Levels Using Biocatalysis Coupled to Assisted Ion Transfer Voltammetry at a Liquid-Organogel Microinterface Array. *Anal. Chem.* **2016**, *88*, 11302−11305.
(20) Yang, L.; Li, Y.; Zhang, Y.; Fan, D.; Pang, X.; Wei, Q.; Du, B. 3D Nanostructured Palladium-Functionalized Graphene-Aerogel Supported Fe_3O_4 for Enhanced $Ru(bpy)_3^{2+}$-Based Electrochemiluminescent Immunosensing of Prostate Specific Antigen. *ACS Appl. Mater. Interfaces* **2017**, *9*, 35260−35267.
(21) Kavosi, B.; Salimi, A.; Hallaj, R.; Amani, K. A Highly Sensitive Prostate-specific Antigen Immunosensor Based on Gold Nanoparticles/PAMAM Dendrimer Loaded on MWCNTS/chitosan/ionic Liquid Nanocomposite. *Biosens. Bioelectron.* **2014**, *52*, 20−28.
(22) Kavosi, B.; Salimi, A.; Hallaj, R.; Moradi, F. Ultrasensitive Electrochemical Immunosensor for PSA Biomarker Detection in Prostate Cancer Cells Using Gold Nanoparticles/PAMAM Dendrimer Loaded with Enzyme Linked Aptamer as Integrated Triple Signal Amplification Strategy. *Biosens. Bioelectron.* **2015**, *74*, 915−923.
(23) Wang, Y.; Li, X.; Lu, G.; Chen, G.; Chen, Y. Synthesis and photo-catalytic degradation property of nanostructured-ZnO with different morphology. *Mater. Lett.* **2008**, *62*, 2359−2362.
(24) Fageria, P.; Gangopadhyay, S.; Pande, S. Synthesis of ZnO/Au and ZnO/Ag Nanoparticles and Their Photocatalytic Application Using UV and Visible Light. *RSC Adv.* **2014**, *4*, 24962−24972.
(25) Dong, Y.; Lin, Q.; Chen, D.; Fu, X.; Wang, M.; Wu, Q.; Chen, X.; Li, S. Amino Acid-Assisted Synthesis of Superparamagnetic $CoFe_2O_4$ Nanostructures for the Selective Adsorption of Organic Dyes. *RSC Adv.* **2013**, *3*, 11628−11633.
(26) He, Y.; Wang, Y.; Yang, X.; Xie, S.; Yuan, R.; Chai, Y. Metal Organic Frameworks Combining $CoFe_2O_4$ Magnetic Nanoparticles as Highly Efficient SERS Sensing Platform for Ultrasensitive Detection of N-Terminal Pro-Brain Natriuretic Peptide. *ACS Appl. Mater. Interfaces* **2016**, *8*, 7683−7690.
(27) Serioa, S.; Silvaa, L. C.; Jorgeb, M. E. M.; Ferreirac, S.; Ciriacoc, L.; Pachecoc, M. J.; Lopesc, A. Ti/Pt/TiO_2 Electrodes Prepared by DC Magnetron Sputtering: Environmental Application on the Degradation of the Acid Orange 7. *Port. Electrochim. Acta* **2017**, *35*, 313−321.
(28) He, Y.; Yang, X.; Yuan, R.; Chai, Y. Switchable Target-Responsive 3D DNA Hydrogels as a Signal Amplification Strategy Combining with SERS Technique for Ultrasensitive Detection of miRNA 155. *Anal. Chem.* **2017**, *89*, 8538−8544.
(29) Wang, Y.; Zhai, J.; Song, Y.; He, L. The Ag Shell Thickness Effect of Au@Ag@SiO_2 Core-Shell Nanoparticles on the Optoelectronic Performance of Dye Sensitized Solar Cells. *Chem. Commun.* **2016**, *52*, 2390−2393.
(30) Long, G. L.; Winefordner, J. D. Limit of Detection. A Closer Look at the IUPAC Definition. *Anal. Chem.* **1983**, *55*, 712A−724A.
(31) Shu, J.; Qiu, Z.; Zhou, Q.; Lin, Y.; Lu, M.; Tang, D. Enzymatic Oxydate-Triggered Self-Illuminated Photoelectrochemical Sensing Platform for Portable Immunoassay Using Digital Multimeter. *Anal. Chem.* **2016**, *88*, 2958−2966.
(32) Farka, Z.; Mickert, M. J.; Hlavaćek, A.; Skladal, P.; Gorris, H. H. Single Molecule Upconversion-Linked Immunosorbent Assay with Extended Dynamic Range for the Sensitive Detection of Diagnostic Biomarkers. *Anal. Chem.* **2017**, *89*, 11825−11830.
(33) Li, J.; Gao, Z.; Ye, H.; Wang, S.; Pierce, M.; Tang, D.; Xia, X. A Non-Enzyme Cascade Amplification Strategy for Colorimetric Assay of Disease Biomarkers. *Chem. Commun.* **2017**, *53*, 9055−9058.
(34) Jang, H. D.; Kim, S. K.; Chang, H.; Choi, J. W. 3D Label-Free Prostate Specific Antigen (PSA) Immunosensor Based on Graphene−Gold Composites. *Biosens. Bioelectron.* **2015**, *63*, 546−551.
(35) Li, J.; Gao, Z.; Ye, H.; Wan, S.; Pierce, M.; Tang, D.; Xia, X. A Non-Enzyme Cascade Amplification Strategy for Colorimetric Assay of Disease Biomarkers. *Chem. Commun.* **2017**, *53*, 9055−9058.
(36) Yang, K.; Hua, Y.; Dong, N.; Zhu, G.; Zhu, T.; Jiang, N. A Novel SERS-based Magnetic Aptasensor for Prostate Specific Antigen Assay with High Sensitivity. *Biosens. Bioelectron.* **2017**, *94*, 286−291.

DOI: 10.1021/acsami.7b19717
ACS Appl. Mater. Interfaces 2018, 10, 15200−15206